3-Benzoylquinoxalinone as a photoaffinity labelling derivative with fluorogenic properties allowing reaction monitoring under “no-wash” conditions

Madeleine Cauwel, Clément Guillou, Kévin Renault, Damien Schapman, Magalie Bénard, Ludovic Galas, Pascal Cosette, Pierre-Yves Renard, Cyrille Sabot

COMMUNICATION

3-Benzoylquinoxalinone as photoaffinity labelling derivative with fluorogenic properties allowing reaction monitoring under "no-wash" conditions

Madeleine Cauwel, [a] Clément Guillou, [b] Kévin Renault, [a] Damien Schapman, [c] Magalie Bénard, [c] Ludovic Galas, [c] Pascal Cosette, [b] Pierre-Yves Renard [a] and Cyrille Sabot,*[a]

Described herein is a quinoxalinone-based photoaffinity probe with caged fluorescence properties. Upon visible blue LED irradiation (λ_{max} 450 nm), this photo-crosslinker is able to covalently capture proteins with concommitant fluorescence labelling. This process enables monitoring applications under "no wash" conditions.

The identification of protein-protein interactions or of biological targets of small-molecule ligands are of prime interest in medicinal chemistry for elucidating new mode of actions of pharmacophores. Important applications are also found in chemical biology for fundamental understanding of cellular functions, or in structural biology for identifying amino acid residues of proteins in contact with ligands.[1]

Methods for identifying biological targets include *in vitro* activity assays, affinity chromatography, [2] activity-based probe (ABP) technology, [3] or photoaffinity labelling (PAL) approach.[4] Whilst the two first approaches rely on the use of isolated proteins or crude cell lysates, in the two latter strategies, interactions from native environments could also be trapped for their subsequent identification. On one hand, the activity-based probes consist of 1) an affinity linker or ligand that favour interactions with the biological target; 2) an electrophilic warhead (such as an epoxide, a Michael acceptor, an activated halogen derivative, or a quinone methide) that reacts covalently and specifically with nucleophilic residues of the active site of the protein target; and 3) a reporter tag such as a fluorophore for identification and purification of modified proteins. This strategy requires finding a fine tuning of the respective reactivity of the two complementary reactive groups, in order to both increase the chance of covalent bond formation once in close proximity, and decrease the signal to noise ratio (if the electrophile reacts with other nucleophilic derivatives). On the other hand, in the affinity labelling (PAL) strategy, the electrophilic warhead is replaced by a more stable photoreactive function which unveiled highly reactive and transient species only upon triggered UV irradiation. These intermediates are able to react covalently with a larger range of residues, not limited to nucleophilic amino acids. As a direct consequence, this strategy has a broader applications spectrum, while avoiding the biased reactivity of ABP towards specific proteins equipped with the required nucleophilic moieties. Traditional photoreactive functions mostly consist of benzophenone, aryl azide, and diazirine group that generate diradical, nitrene, and carbene intermediate, respectively, when exposed to 280-365 nm UV irradiation. The access to functionalized chemical probes bearing a photoreactive function, a ligand, and a fluorophore is synthetically challenging, and the presence of a bulky fluorophore may disrupt protein-ligand interactions, and generally low photo-crosslinking yields, which further complicates the isolation and identification of the photo-crosslinked species. To address this point, minimalist probes were recently designed, in which the fluorophore was elegantly replaced by a discrete bioorthogonal handle (*i.e.* terminal alkyne, cyclopropene), that was used to install the fluorescent tag once the photocrosslinking of ligand-protein interactions was achieved.[5-7] However, this strategy requires a two-step protocol: 1) the photolabelling step to ensure the integrity of the ligand-protein complex during its isolation; 2) a bioorthogonal reaction for installing the fluorescent tag. This approach can also produce background fluorescence due to the presence of residual fluorescent tag typically used in excess, which prevents, among others, real-time monitoring applications. An alternative, yet underexplored approach, consists in using fluorogenic photoreactive functions which are able to both photocrosslink and unveil a fluorescent scaffold in a single-step process. This approach has been combined with diazo-,[8] azide-[8-11] and diazirine-based photoreactive functions.[12-13] This strategy was extended to the photoreactive diaryltetrazole function, which has shown to preferentially react with aspartic acid and glutamic acid residues of proteins through the formation of a nitrile imine intermediate.[14] However, 280 and 300 nm UV irradiation are required to photoactivate aryl azides and diaryltetrazoles, respectively, which can induce severe damage to biological systems.

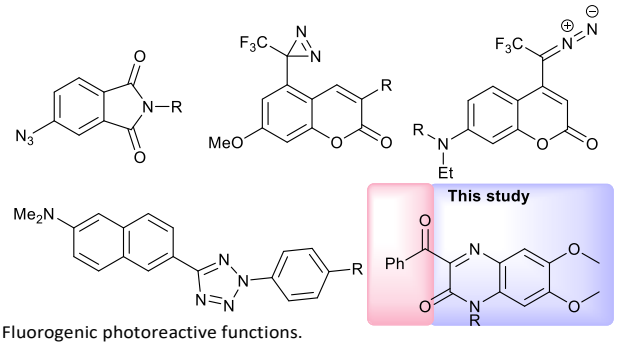

Fig. 1 Fluorogenic photoreactive functions.

Among the usual photo-crosslinkers, the benzophenone class of compounds is scarcely represented yet, only a photo-crosslinking system with uncaged fluorescence properties has been reported. In this system, the aryl ketone group was incorporated into a bulky BODIPY fluorophore.[15] A small fluorogenic diaryl ketone-based photoreactive function would be, however, particularly useful for the direct and real-time monitoring of photo-affinity crosslinking through concomitant fluorescent labelling experiments. In fact, aryl azide and diazirine derivatives generate irreversibly reactive intermediates upon UV activation that react with surrounding water molecules in the absence of nearby biological targets, leading to a fluorescence recovery.[12] On the other hand, once photo-activated, benzophenone derivatives yield diradical intermediates, which either react with the desired target, or react reversibly with water molecules, thus preventing the formation of a fluorescent product in the absence of nearby protein target.[16]

Herein, we report the use of a benzophenone-quinoxalinone hybrid system for the fluorogenic photoaffinity labelling of protein targets. As an additional bonus, the labelling reaction could proceed above 400 nm, conditions that are less detrimental for the protein structures.[17]

We recently reported that 3-benzoyl-6-methoxyquinoxalin-2(1*H*)-ones such as compound **1** exhibited dramatic fluorescence turn-on upon $NaBH_4$ reduction of the ketone moiety into the corresponding alcohol (Figure 2A).[18] The presence of the ketone moiety is responsible for the fluorescence quenching, presumably through singlet-to-triplet intersystem crossing process, a non-radiative de-excitation pathway which competes with the fluorescence phenomenon.[18] From these studies, it is therefore expected that the transformation of the carbonyl group during photoaffinity labelling reactions would also lead, to some extent, to fluorescence recovery. However, the access to **1** required the separation of isomeric 7-methoxy- and 8-methoxy-benzodiazepinone intermediates at the N-methylation step. Accordingly, we decided to prepare the 6,7-dimethoxyquinoxalinone analogue **3**, thus avoiding the formation and troublesome separation of isomeric intermediates. Compound **3** was prepared in a total of 3 steps in 29% overall yield from readily available 4,5-dimethoxy-1,2-phenylenediamine. The synthetic strategy relies on the ring contraction of benzodiazepine-2-ones we previously described mediated by *N*-bromosuccinimide in the presence of DMSO, which serves both as a solvent and an oxidant.[19]

Then, the carbonyl to hydroxyl fluorescence turn-on ability of 3-benzoylquinoxalinone **3** functionalized by two electron-donating methoxy substituents was investigated. As expected, the treatment of **3** by $NaBH_4$ resulted in a remarkable 100-fold fluorescence enhancement. This was also consistent with the values of the fluorescence quantum yields of **3** and **4**, which were determined to be <0.01 and 0.35 in PBS pH 7.4, respectively. Importantly, compound **3** possesses a large absorption band with a maximum at 402 nm, which will allow to irradiate quinoxalinone probes in the visible region (Figure S4), thus limiting the photodamages induced by <350 nm irradiations. To investigate the benzophenone-like behaviour of such benzoylquinoxalinones upon irradiation, similarly prepared compound **5** (bearing an ester moiety useful for future functionalization) was photoexcited by a visible blue LED light (λ_{max} 450 nm) in neat pyrrolidinone (or in mixture with water), which was used as a simple amide-containing the peptide linkage. The expected crosslinked product **6** was not formed, but instead compound **7** lacking the benzoyl group was obtained as the only fluorescent product (Figures 2B and 2C). Two plausible mechanisms were proposed involving either a Norrish Type I photochemical cleavage of **5**, or the formation of a diradical of imine at first step (Figure S33 and S34 for mechanistic details).

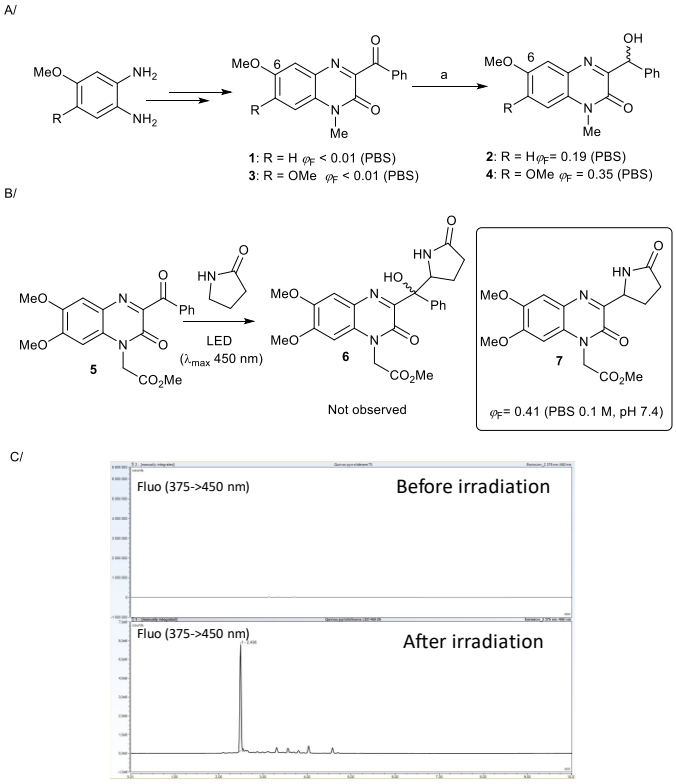

Fig. 2 A/ Preparation of 3-benzoylquinoxalinone **1** and **3** and hydroxyl-containing quinoxalinone **2** and **4**. Reagents and conditions: (a) $NaBH_4$, MeOH, r.t. for 10 min., (98%, **2**; quant., **4**); B/ Photoreaction of quinoxalinone **5** with pyrrolidinone under a visible blue LED light (λ_{max} 450 nm) for 2h; C/ RP-HPLC fluorescence chromatograms obtained before and after irradiation of **5** in pyrrolidinone (λ_{ex} 375 nm, λ_{max} 450 nm).

Following this preliminary study, the fluorescent labelling of bovine carbonic anhydrase II (CA-II, molecular weight 30 kDa)

used as a model target protein, was investigated. From quinoxalinone **5**, a two-step ester hydrolysis/amidation sequence was carried out to introduce the 4-sulfamoyl benzylamine ligand, which belongs to a well-established family of CA-II inhibitors, leading to the probe **8**.[20] In order to investigate the influence of the chain length on the labelling efficiency, probe **9**, in which the ligand is separated by two PEG units from the photoreactive quinoxalinone scaffold, was also accordingly prepared (Scheme 2, see ESI for experimental details).

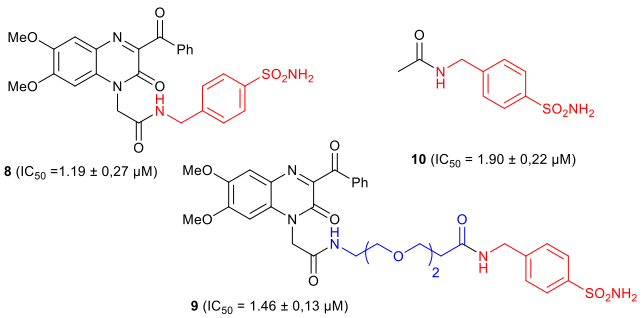

Scheme 2 Preparation of modified quinoxalinones **8** and **9**.

These compounds in hands, their IC_{50} values were determined, and found to be 1.19 µM and 1.46 µM for **8** and **9**, respectively. These values are in agreement with the one found for the parent compound benzylamide **10** (IC_{50} = 1.90 µM), thus demonstrating that the 3-benzoylquinoxalinone scaffold does not significantly interfere with the binding properties of **10**, whatever the chain length. The photo-crosslinking and concomitant fluorescence labelling of bovine CA-II (10 µM) with probes **8** and **9** was conducted in PBS pH 7.4 under visible blue LED irradiation (λ_{max} 450 nm). The photoaffinity labelling could be followed by fluorescence spectroscopy (λ_{ex} 375 nm) under "no-wash" conditions, that is, without filtering the excess of unreacted probe. In fact, no fluorescence increase was observed when the 3-benzoyquinoxalinone is irradiated for 1h in PBS pH 7.4 (Figure S12). In contrast, as shown in Figure 3A-a and -b, probes **8** and **9** showed a noticeable 10- and -3 fold increase, respectively, in fluorescence at 460 nm upon binding to the protein. The labelling efficiency with probe **8** was found to be about 2% (Figure S19). Most of the labelling was achieved after 15 min and 3 min of irradiation with visible blue LED (λ_{max} 450 nm) and under near UV LED (λ_{max} 405 nm), respectively (Figures S14-16).

Control experiments carried out with **3** containing only the photoreactive part of the probe (Figure 3A-c), or with probe **8** in the presence of CA-II inhibitor, acetazolamide (10 equiv., Figure 3A-d), showed, however, no significant fluorescence increase. These results indicate the specificity of the labelling. Of note, two emission peaks at 460 and 560 nm were observed for quinoxaline derivatives in aqueous systems. Complementary photophysical studies suggest that one of the two peaks may correspond to that of aggregates of quinoxalinone molecules. In fact, only one fluorescence emission band was observed in the organic solvent DMSO, in which quinoxalinones are well soluble (Figure S8).

Moreover, gel electrophoresis analyses further confirmed the fluorescence labelling of CA-II specifically with **8** and under light irradiation stimulus, with the presence of a fluorescent band in the 30 kDa region (Figure 3B, lane 2).

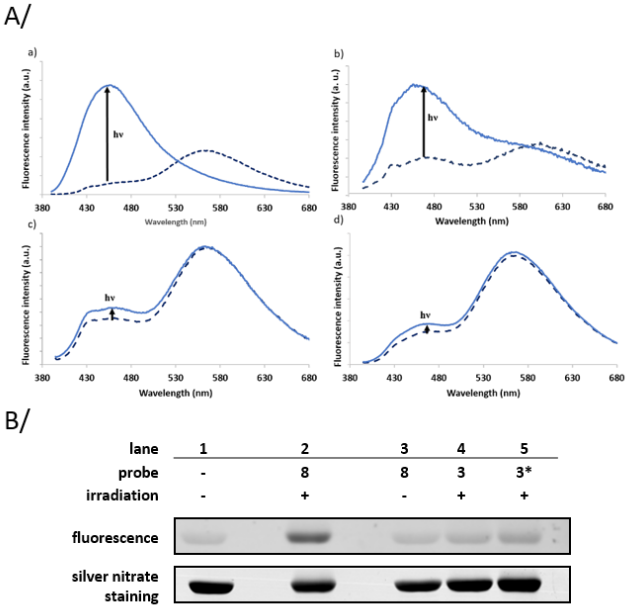

Fig. 3 A/ Fluorescence emission spectra of a mixture of CA-II (10 µM = 0.3 mg/mL) with different probes (10 µM, 1 eq.) (λ_{ex} 375 nm) in water at 25°C, before (dashed line) and after (solid line) 1 h of blue LED light irradiation: (a) probe **8**; (b) probe **9**; (c) quinoxalinone **3**; (d) 30 min pre-incubation with known CA-II inhibitor acetazolamide (100 µM, 10 eq.) before introducing probe **8**. **B/** SDS-PAGE analysis of CA-II (30 kDa). Conditions: **8** (10 µM), **3** (10 µM), CA-II (10 µM = 0,3 mg/mL) in water and LED blue light irradiation (1 h). *30 min pre-incubation with known CA-II inhibitor acetazolamide (100 µM, 10 eq.) before introducing probe **8** (10 µM). In-gel fluorescence imaging (λ_{ex} = 302 nm, λ_{em} > 535 nm).

The labelling specificity was further investigated by tagging the bovine CA-II mixed with human blood plasma (HBP, Figure 4). Similarly, CA-II was efficiently fluorescently labelled by probe **8**, while only light fluorescence for CA-II was detected with the non-specific probe **3**. In the absence of irradiation, no labelling was observed with **8**, confirming this probe provides spatial and temporal control over reactivity.

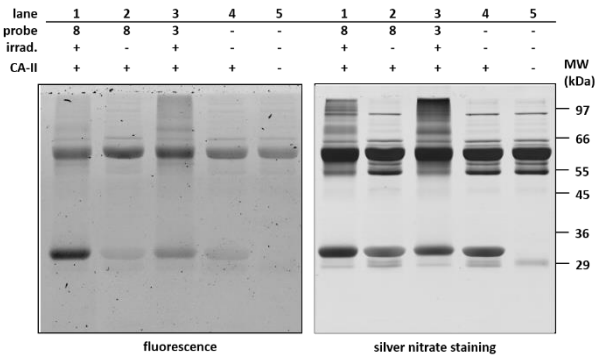

Fig. 4 Specific fluorescence labelling of CA-II (30 kDa) by **8** in the presence of human blood plasma. Conditions: **3** (100 µM) or **8** (100 µM), CA-II (100 µM = 3 mg/mL), human blood plasma diluted by 10 in PBS pH 7.4 and visible blue LED light irradiation (2 h). In-gel fluorescence imaging (λ_{ex} = 302 nm, λ_{em} > 535 nm).

Encouraged by these results, the fluorescence turn-on properties of quinoxalinones was next investigated in a more complex medium, through the fluorescent labelling of cells under "no-wash" conditions. To illustrate that proof-of-principle, the functionalizable quinoxalinone **5** was equipped with a phospholipid, 1,2-dioleoyl-sn-glycero-3-phosphoethanolamine known to interact with biological membranes, yielding phospholipid-based probe **11**, in order to specifically visualize lipid-rich organelles that are abundant in cells (Figure 5).[21,22] After incubation of fixed cells with probe **11** and visible blue LED irradiation, both for 1 h, confocal microscopy showed a concentration-dependent effective labelling of most, if not all, PC12 cells (Figure 5). Satisfyingly, significantly lower fluorescence was observed in the control experiment carried out in the absence of irradiation (Figure 5B). In addition, higher magnifications revealed subcellular positive elements suggesting that endomembranes around the nuclear membrane as well as membranes of intracellular vesicles are labelled with probe **11**.

Fig. 5 A. Labelling cells with irradiated probe **11** (10^{-3} M). Scale Bar = 50 µm B.

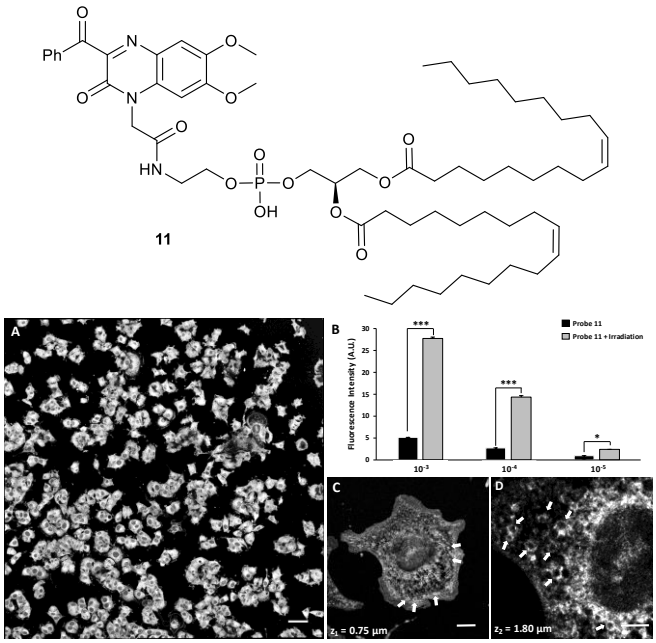

Influence of probe concentration. ***, p<0.001, statistical significance versus probe **11** without irradiation; *, p<0.05, statistical significance versus probe **11** without irradiation. C,D. Confocal images at different z position (z1 and z2). Scale Bar = 10 µm (C), Scale Bar = 5 µm (D). White arrows indicate labelled membrane of intracellular vesicles.

In summary, an easy photolabelling procedure in the presence of compact quinoxalinone derivatives playing the role of both the photoreactive function and pro-fluorophore, is reported. Advantageously, the labelling proceeds effectively under visible blue LED, conditions that are less photo-damaging to proteins and cell contents than traditionally used UV irradiations. The use of carbonyl-conjugated quinoxalinone systems possessing photocrosslinking ability accompanied with caged-fluorescence properties enables direct monitoring of the fluorescence labelling, that is, without removing the excess of unreacted probe. This was leveraged for the fluorescent labelling of endomembrane systems of cells by using a photoreactive phospholipid probe. This proof-of-concept being established, 3-benzoylquinoxalinone-based probes will be used for identifying new protein-protein interactions occurring in specific subcellular organelles, and results will be published in due course.

This work was supported by the Region Normandie, and a PhD financial support to MC. This work was also partially supported by the Centre National de la Recherche Scientifique (CNRS), the INSA Rouen, Rouen Normandy University, The Institute of Research and Innovation in Biomedicine (IRIB), and the Labex SynOrg (ANR-11-LABX-0029). We also thank Laetitia Bailly (INSA Rouen) and Emilie Petit (INSA Rouen) for HPLC-MS analyses and Albert Marcual (CNRS) for HRMS analyses.

Conflicts of interest

"There are no conflicts to declare".

Notes and references

1 E. L. Vodovozova, *Biochem (Mosc)*, 2007, **72**, 1-20.
2 D. V. Titov and J. O. Liu, *Bioorg. Med. Chem.*, 2012, **20**, 1902-1909.
3 E. Smith and I. Collins, *Future Med. Chem.*, 2015, **7**, 159-183.
4 H. Guo and Z. Li, *Medchemcomm.*, 2017, **8**, 1585-1591.
5 Z. Li, P. Hao, L. Li, C. Y. Tan, X. Cheng, G. Y. Chen, S. K. Sze, H. M. Shen and S. Q. Yao, *Angew. Chem., Int. Ed.*, 2013, **52**, 8551-8556.
6 Z. Li, D. Wang, L. Li, S. Pan, Z. Na, C. Y. Tan and S. Q. Yao, *J. Am. Chem. Soc.*, 2014, **136**, 9990-9998.
7 S. Kellner, S. Seidu-Larry, J. Burhenne, Y. Motorin and M. Helm, *Nucleic Acids Res.*, 2011, **39**, 7348-7360.
8 S.-Y. Dai, D. Yang, *J. Am. Chem. Soc.*, 2020, **40**, 17156–17166.
9 E. Păunescu, L. Louise, L. Jean, A. Romieu and P.-Y. Renard, *Dyes Pigm.*, 2011, **91**, 427-434.
10 K. Chiba, M. Asanuma, M. Ishikawa, Y. Hashimoto, K. Dodo, M. Sodeoka and T. Yamaguchi, *Chem. Commun.*, 2017, **53**, 8751-8754.
11 K. Chiba, Y. Hashimoto and T. Yamaguchi, *Chem. Pharm. Bull.*, 2017, **65**, 994-996.
12 T. Tomohiro, A. Yamamoto, Y. Tatsumi and Y. Hatanaka, *Chem. Commun.*, 2013, **49**, 11551-11553.
13 T. M. Ayele, S. D. Knutson, S. Ellipilli, H. Hwang and J. M. Heemstra, *Bioconjugate Chem.*, 2019, **30**, 1309-1313.
14 Z. Li, L. Qian, L. Li, J. C. Bernhammer, H. V. Huynh, J. S. Lee and S. Q. Yao, *Angew. Chem., Int. Ed.*, 2016, **55**, 2002-2006.
15 D. P. Murale, S. C. Hong, J. Yun, C. N. Yoon and J. S. Lee, *Chem. Commun.*, 2015, **51**, 6643-6646.
16 G. Dorman, H. Nakamura, A. Pulsipher and G. D. Prestwich, *Chem. Rev.*, 2016, **116**, 15284-15398.
17 D. I. Pattison, A. S. Rahmanto and M. J. Davies, *Photochem. Photobiol. Sci.*, 2012, **11**, 38-53.
18 K. Renault, P.-Y. Renard and C. Sabot, *New J. Chem.*, 2017, **41**, 10432-10437.
19 H. Mtiraoui, K. Renault, M. Sanselme, M. Msaddek, P. Y. Renard and C. Sabot, *Org. Biomol. Chem.*, 2017, **15**, 3060-3068.
20 C. B. Mishra, S. Kumari, A. Angeli, S. M. Monti, M. Buonanno, M. Tiwari and C. T. Supuran, *J. Med. Chem.*, 2017, **60**, 2456-2469.
21 J. Yang, J. Seckute, C. M. Cole and N. K. Devaraj, *Angew. Chem., Int. Ed.*, 2012, **51**, 7476-7479.
22 X. Ji, K. Ji, V. Chittavong, R. E. Aghoghovbia, M. Zhu and B. Wang, *J. Org. Chem.*, 2017, **82**, 1471-1476.